Geomagnetic Indices Forecasting and Ionospheric Nowcasting Tools

GIFINT

Executive summary

Ref: Contract no. 17032/03/NL/LvH

Doc. No.:**GIFINT/executive_summary**
Issue: **1**
Revision: **0**
Date: **07/11/2007**

Table of Contents

1. RATIONALE

In the framework of space weather an important role is played by magnetospheric storms and substorms. During magnetospheric storms intense fluctuations of the horizontal component of the ground magnetic field are observed (Gonzalez et al., 1994), which are globally characterised through the Dst index. Magnetospheric substorms are characterised by large enhancements of the auroral electrojet and can be described through the AE (Auroral Electrojet) index. The state of the near-Earth space plasma affects the reflection and transmission of radio waves in the ionosphere. Therefore, especially under disturbed conditions, nowcasting of the principal ionospheric parameters is useful for space weather purposes and can be addressed by global and regional models based on real time ionospheric measurements.

On the basis of these considerations, a service has been developed, for the GIFINT users (see Section 7) and for the space weather community at large, aiming at: a) developing new ANN (Artificial Neural Network) algorithms to forecast the Dst and AE indices with 1 hour resolution based on L1 ACE solar wind measurements; b) developing Ionospheric Nowcasting Tools (INT) for the real-time mapping of the foF2 and M(3000)F2 parameters over the Central Mediterranean area; c) assessing the quality of such tools through post-event analysis. All the GIFINT products are continuously displayed in real time through a web site (http://gifint.ifsi-roma.inaf.it). The GIFINT scientific results have been presented in a number of scientific conferences and published in several papers (Pallocchia et al., 2006; Amata et al., 2007a; Amata et al., 2007b; Cid et al, 2007; Pallocchia et al., 2007).

2. TECHNICAL DEVELOPMENT OF THE PROJECT

2.1 *DST* FORECASTING

All past algorithms for *Dst* forecasting make use of both plasma and IMF data (Amata et al., 2007, and references therein). GIFINT also developed and tested several such algorithms. However, the dependence on plasma parameters poses a serious operational constraint (as seen during the Halloween 2003 storms). In fact, in conjunction with large emissions of particles and radiation from the Sun, the solar wind plasma instruments can saturate for time periods lasting for hours or even days. On the contrary, magnetometers are not affected by such transitory malfunctions; moreover, their operational life is far longer than that of plasma instruments. Therefore, we developed an ANN Elman (Elman, 1990) algorithm based on IMF only, call hereafter EDDA (Empirical *Dst* Data Algorithm), which has 3 inputs (B_z, B^2, B_y^2), 4 context units, 1 hidden layer with 4 neurons with a hyperpobolic tangent transfer function, 1 linear output neuron. The input parameters are hourly averages calculated from L1 IMF data in GSM coordinates. The output is assigned the time t + 1 for inputs at the time t to account for the 1 hour average travel time of the solar wind from L1 to the Earth's magnetopause.

The data base used by GIFINT consists of WIND and ACE L1 IMF hourly averages from 1995 to 2002 (amounting to nearly 64000 hourly averages). From this a training set was extraced, comprising of about 6000 hourly averages, including both disturbed and quiet periods; the rest of the data base was used as a test set. Several algorithms were then trained. Finally, they were all run over the whole test set and the algorithm which performed best was chosen as the final algorithm (linear correlation coefficient 0.83; total root mean square error 13.9 nT over the whole test set).

2.2 AE FORECASTING

At the start of the GIFINT activities, we trained a four input (B_z, B, n and V_x) Elman ANN algorithm for the forecasting of 1-hour averages of AE based on a training test built from 1978 and 1979 OMNI data. Later on, many more tests were performed after selecting a training and a testing data set suitable for the development of an operational AE forecast algorithm. This was done according to the following criteria: 1) use solar wind data taken from a single spacecraft, 2) use solar wind data measured at L1. These conditions restricted the data base to the whole of 1995, which is the last year for which provisional AE data were available and the first year of WIND operation at L1. Having chosen to use L1 data, 1 min WIND data were propagated ballistically to Earth. Then, we averaged AE and solar wind data over 5, 15, 20, 30, 60 min, so as to build time consistent data sets of averaged AE and solar wind data.
Starting from the 60 min data set, we trained several ANN Elman algorithms, with different complexity and various inputs, and compared their performances. Eventually, the following ANN structure was selected: 2 inputs, B_z and V_x, four hidden neurons (with a hyperbolic tangent transfer function), four context units, one output neuron (with an exponential transfer function). We then developed 5 ANN algorithms, based on 5, 15, 20, 30 and 60 min averages of AE and solar wind data and compared their performances by considering single events and from a statistical point of view. The study of single events showed that AE variations on time scales of 5-10 min are not reproduced, while variations on time scale longer than 1 hour are reproduced, although with smaller peak values than for AE. For the statistical study, we considered the total normalised standard deviation, R, between the forecast and the Kyoto AE as a function of AE averaging time and found that it decreases exponentially with averaging time, so that R(60min) differs from the asymptote $R(\infty)$ by 3% only. These results can be interpreted in terms of the contribution of the two known AE components (Pallocchia et al., 2007): the solar wind driven, which could be responsible for the broader enhancements, and the unloading component which could be responsible for the smaller scale large peaks, which fail to be reproduced by the AE ANN algorithms. The fact that the peaks of the broader enhancements are underestimated suggests that the separation between the two components is not complete at these time scales. In conclusion, it is possible to qualitatively forecast AE enhancements on time scales of a few hours bearing in mind that an underestimate of peak values by a factor of 1.5–2 is very probable, while faster variations of AE, over time scales below 60 min, cannot be reproduced. As such, there is no point in running on real time AE forecasts on time scales shorter than an hour. Moreover, no post-event analysis for the AE index has been made because neither the final nor the provisional Kyoto AE indices are available for the period during which GIFINT was operational. The 60 min AE with B_z and V_x inputs is currently displayed in the GIFINT web site. The output is assigned the time t + 1 for inputs at the time t to account for the 1 hour average travel time of the solar wind from L1 to the Earth's magnetopause.

2.3 THE INT PRODUCTS

For the INT products GIFINT made use of SIRMUP, which is based on Improved SIRM (Simplified Ionospheric Regional Model). Improved SIRM is a regional ionospheric model of the standard vertical incidence ionospheric characteristics developed by the COST 238 project (Bradley, 1995), and applied to a more extended area taking into account the influence of high latitude regions (Zolesi et al., 1993, 1996). According to the SIRM updating method (SIRMUP) local real time values of foF2 can be determined from the SIRM model by using an effective

sunspot number, R_{eff}, instead of the 12-month smoothed sunspot number, R_{12} (Zolesi et al. 2004). For that purpose, R_{eff} is obtained from the best fit between model calculation and actual measurements by a grid of ionosondes located in the mapping area. INT provides the SIRMUP 1-hour resolution nowcasting maps of foF2 and M(3000)F2 over Italy (i.e. the region of interest to GIFINT users). At first R_{eff} was calculated from real time automatically scaled ionograms provided by the Rome station (41.9N; 12.5 E), but, more recently, data from a second station, located in Sicily (38.0 N; 14.0 E), were used together with the Rome ones.

2.4 THE POST EVENT ANALYSIS

2.4.1 Summary of the EDDA performance

The EDDA algorithm has been compared with two recent algorithms (which make use of both IMF and plasma data): the first one (called "Lund" hereafter) also based on the ANN technique (Lundstedt et al., 2002); the second one (called "Wang" hereafter) based on differential equations (Wang et al., 2003). For that purpose, the percent root mean square error was calculated for EDDA, Lund and Wang, between the beginning of 2003 and May 15, 2005, for 25 nT bins of Dst, as a quantitative tool to assess the algorithm performance. Fig. 1 shows that, in the (0, 25nT) bin, *R* has a maximum of 100, 118, and 140 for Wang, EDDA and Lund respectively. Moving towards more negative Dst values, we see that *R* drops to around 40 in the (-50nT,-25nT) bin, roughly corresponding to "small" storms, being the Lund value somewhat higher and the Wang value lower. As Dst decreases further, we see that *R* is generally higher for the Lund algorithm. EDDA has values comparable to the Wang ones between -75 and -175 nT, somewhat higher between -175 and -325 nT, and slightly lower between -325 and 425 nT. The comparison between the three algorithms was also made by considering several magnetospheric storms. In general, the thee algorithms perform similarly for small and moderate storms, while EDDA and Wang perform better than Lund for intense and severe storms. In conclusion, EDDA has the advantage with respect to Wang that the reliability of its output is not influenced by the lack of correct plasma data during disturbed periods. In the unlikely case of an IMF data gap lasting for more than 1 hour, it has been found that the EDDA output will retrieve its full performance within the next 4-5 prediction points.

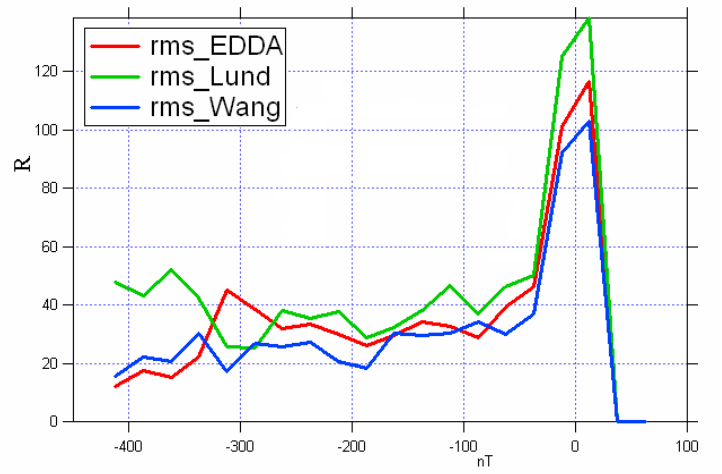

Fig. 1. Percent root mean square error for EDDA, Lund and Wang.

2.4.2 The August 2004 storm

We now consider the storm period from 29 August to 2 September 2004 both as regards the GIF and the INT tools (Fig. 2). The top panel displays, from top to bottom: the three IMF components in GSM (in units of 0.1 nT; x in red, y in green, z in blue), the magnetic field intensity (in units of 0.1 nT; violet line), the particle number density (in units of .1 cm^{-3}; cyan line), the solar wind V_x (black line), the Kyoto Dst (in red) and the Edda Dst (in black). The three IMF components are shifted by 100 nT. V_x is shifted by -300 km/s. An interplanetary shock flew past ACE at ~ 0930 UT on August 29 with a magnetic field jump from ~ 4 to ~7 nT. The shock was followed by interplanetary ejecta, which may be related to a CME detected by LASCO/SOHO on August 27 at ~0930 UT. The IMF becomes southward at ~ 04 UT on August 30 and reaches the minimum value (-15 nT) at ~ 22 UT; then, it remains slightly southward during the next two days. Correspondently, a moderate storm develops with a minimum Dst value of –100 nT at 22 UT and a slow recovery phase. The EDDA algorithm well reproduces the minima, both in time and in amplitude, and the recovery phase.

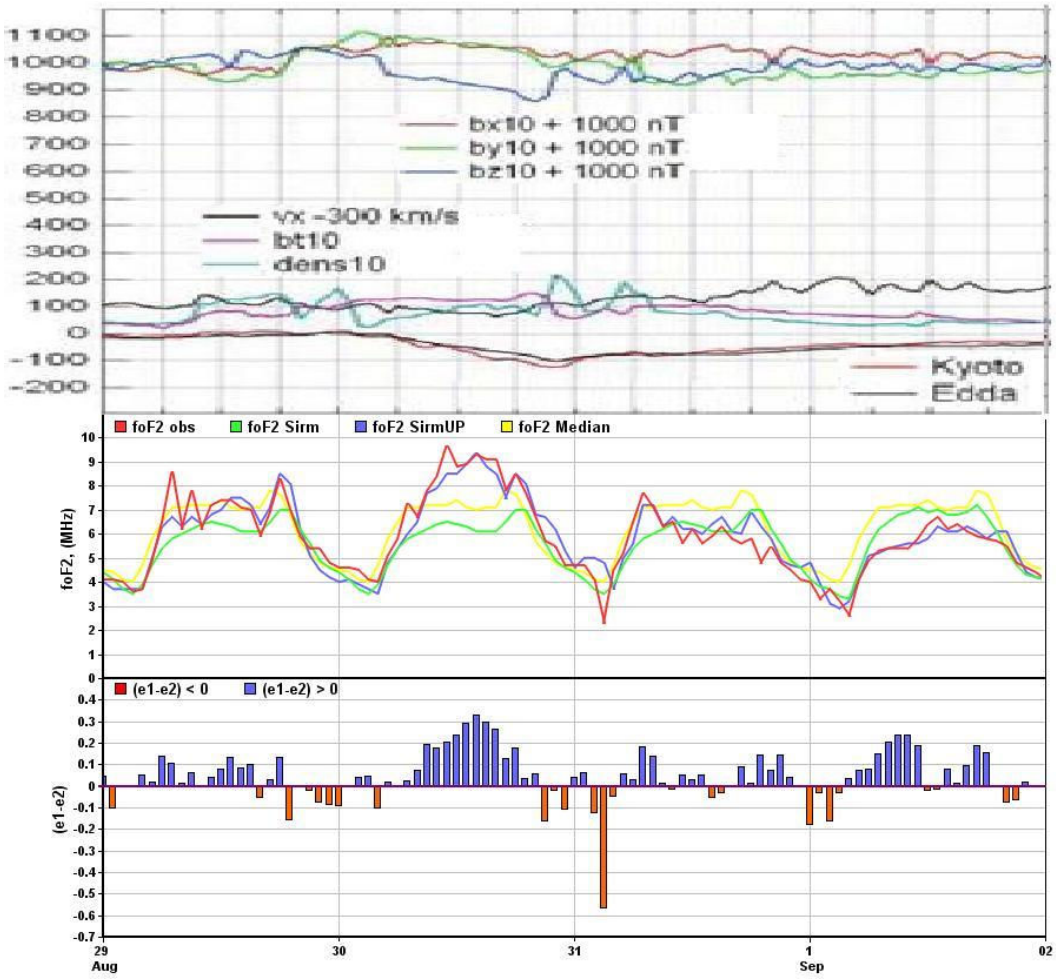

Fig. 2. August 29 – September 2, 2004. Top panel: Kyoto and EDDA Dst and L1 IMF and plasma data. Central panel: simulated and observed foF2. Bottom panel: (e1-e2) parameter.

The Fig. 2 central panel displays foF2 observed at the San Vito (40.6°N; 17.8°E) test station (red line) together with the foF2 predicted by SIRM (green line) and by SIRMUP (blue line), based on R_{eff} calculated from autoscaled values coming from the San Vito and Rome digisondes. The monthly median values of foF2 are also shown (yellow line) for reference. Finally, the bottom panel shows the (e_1-e_2) parameter, which is expected to be positive when the real-time updating is successful. We notice that the observed foF2 clearly differs from the median foF2 between 09 and 17 UT on 30 August by more than 2 MHz, when the Dst was falling. In that period the SIRMUP nowcast reproduces the observations reasonably well, while the SIRM nowcast fails to do so.

As a final consideration we remark that this event well describes how the GIF and INT tools can be used in a coordinated way: the Edda algorithm provides the forecast of the geomagnetic storm and the SIRMUP model provides the correct foF2 and M(300)F2 at the times when the observed values depart from the median values.

3. COST AND BENEFIT ANALYSIS AND USER SATISFACTION

The GIFINT contribution to the cost and benefit analysis has been delivered in written to SEA (the company charged by ESA to independently assess the costs and benefits of the Space Weather Pilot Project) through three documents: Provider Survey document, filled in by GIFINT, User Survey document filled in by the TELDIFE user, User Survey document filled in by the Protezione Civile user.

4. BUSINESS PLAN AND FUTURE APPLICATIONS

After the end of the ESA Pilot Project (April 1st 2006) GIFINT has continued to operate thanks to a small funding by the Italian Space Agency (ASI), which has ended on September 26th 2007. GIFINT is seeking further funding from ASI. If new funding will be available, GIFINT would perform the following activities over a one year period: - update the evaluation of the Dst and AE forecasts and of the INT nowcasts; - develop a new Dst algorithm taking advantage of the new experimental data after 2002; - extend the INT tools to a limited area of the southern hemisphere by making use of a new digital ionosonde already installed by INGV in Argentina. The requirement for continuing the GIFINT activities is that the ACE L1 data on which they are based continue to be available to GIFINT.

A future improvement of the Dst forecast could be obtained by running on real time the Dst algorithm on the DPU of a new solar wind monitor (as ACE was not designed for that). A considerable improvement could be achieved by placing the solar wind monitor closer to the Sun along the Sun-Earth line (e.g. 500 R_E would allow a 3 hours forecast). However, new orbital techonologies should be developed (e.g. solar sails)

As regards, the INT tools, they make use of proprietary data of INGV which should continue to be available in the next years as long as its digital ionosondes are in operation. As regards the possibility to increase the INT value, this could be obtained by extending the area covered by the nowcast (e.g. from Italy to Europe).

5. THE GIFINT ORGANIZATION AND USERS

GIFINT (lead by Dr. E. Amata, IFSI) coordinated the work of 16 researches (belonging to five scientific institutions: IFSI-INAF, INGV and Un. De l'Aquila in Italy; CCRLR in the UK; NOA in Greece) distributed in three Work Packages (WP). WP100 (lead by Dr. G. Consolini, IFSI) and

WP200 (lead by Dr. B. Zolesi, INGV) developed the Dst and AE forecasting and INTs, respectively. WP300 (lead by Dr. E. Amata, IFSI) was devoted to the post-event analysis of the performance of the WP100 and WP200 tools during the GIFINT operation.

The GIFINT users were: **TELEDIFE,** Direzione Generale delle Telecomunicazioni, dell'Informatica e delle Tecnologie Avanzate del Ministero della Difesa, Roma, Italy; **Dipartimento per la Protezione Civile**, Ministero degli affari interni, Roma, Italy.

6. REFERENCES

Amata, E., Pallocchia, G., Consolini, G., Marcucci, M. F., Bertello, I., Comparison between three algorithms for Dst predictions over the 2003-2005 period, JASTP, in press, 2007a.

Amata, E., Pallocchia, G., Consolini, G., Marcucci, M. F., Can the AE index be forecast?, COST 724 final report, OPOCE, in press, 2007b.

Bradley, P. A., COST 238 Final Report, Commission of the European Communities, Ratherford Appleton Laboratory, Chilton Didcot, 1995.

Cid, C., Amata, E., Cerrato, Y., Pallocchia, G., Consolini, Saiz, , E., Forecasting Dst from solar wind data, COST 724 final report, OPOCE, in press, 2007.

Elman, J. L.: Finding structure in time, Cognitive Sci., 14, 179–211, 1990.

Gonzalez, W. D., Joselyn, J. A., Kamide, Y., Kroehl, H. W., Rostoker, G., Tsurutani, B. T., and Vasyliunas, V. M., What is a geomagnetic storm?, J. Geophys. Res., 99, 5771–5792, (1994).

Lundstedt, H., Gleisner, H., and Wintoft, P.: Operational forecasts of the geomagnetic Dst index, Geophys. Res. Lett., 29, 34–1, 2002.

Pallocchia, G., Amata, E., Consolini, G., Marcucci, M.F., Bertello, I., Geomagnetic Dst index forecast based on IMF data only, Ann. Geoph., 24, 989-999, (2006).

Pallocchia, G., Amata, E. Consolini, G., Marcucci, M.F., Bertello, I.: AE index forecast at different time scales through an ANN algorithm based on L1 IMF and plasma measurements. JASTP, In press (2007).

Wang, C. B., Chao, J. K., and Lin, C.-H., Influence of the solar wind dynamic pressure on the decay and injection of the ring current, J. Geophys. Res., 108, 51, 2003.

Zolesi, B., Lj.R. Cander, and G. de Franceschi, Simplified ionospheric regional model for telecommunication applications, Radio Sci., 28(4), pp. 603-612, 1993.

Zolesi, B., Lj.R. Cander and G. de Franceschi, On the potential applicability of the simplified ionospheric regional model to different mid-latitude areas, Radio Sci., 31(3), pp. 547-552, 1996.

Zolesi, B., A. Belehaki, I. Tsagouri, and Lj.R. Cander, Real-time updating of the Simplified Ionospheric Regional Model for operational applications, Radio Sci., 39(2), RS2011 10.1029/2003RS002936, 2004.